

# Crystallographic and Thermodynamic Comparison of Natural and Synthetic Ligands Bound to Streptavidin

P. C. Weber,\* J. J. Wendoloski,<sup>†</sup> M. W. Pantoliano, and F. R. Salemme<sup>†</sup>

Contribution from The Du Pont Merck Pharmaceutical Company, P.O. Box 80228, Wilmington, Delaware 19880-0228. Received July 11, 1991

**Abstract:** The thermodynamic parameters of binding biotin and the dye 2-(4'-hydroxyphenylazo)benzoic acid (HABA) to streptavidin have been determined and are compared, together with X-ray crystal structures of the protein–ligand complexes and apstreptavidin. The X-ray crystal structures of apstreptavidin (space group *I*222, *a* = 94.2 Å, *b* = 104.0 Å, *c* = 47.7 Å, crystallographic *R*-factor = 0.209 at 1.84 Å resolution), a streptavidin–biotin complex (*I*222, *a* = 95.6 Å, *b* = 105.5 Å, *c* = 47.2 Å, *R*-factor = 0.171 at 1.55 Å resolution), and a streptavidin–HABA complex (*I*222, *a* = 95.1 Å, *b* = 105.6 Å, *c* = 47.4 Å, *R*-factor = 0.185 at 1.78 Å resolution) show common aspects of solvent displacement from the protein binding site together with preservation of an important interaction where the biotin ureido and HABA carboxylate oxygens bind in an oxyanion pocket formed by oriented hydrogen-bond donors in the binding site. Nevertheless, titrating calorimetric measurements show that biotin binding is enthalpically favored ( $\Delta G^\circ = -18.3$  kcal/mol,  $\Delta H^\circ = -32.0$  kcal/mol), while entropy terms dominate HABA binding ( $\Delta G^\circ = -5.27$  kcal/mol,  $\Delta H^\circ = 1.70$  kcal/mol).

## Introduction

New pharmaceuticals are typically developed through screens that select active leads from a large compound library. In most cases, little is known about how interactions of a lead compound compare with those of the natural ligand bound to the target receptor. To investigate how dissimilar ligands are accommodated by a common binding site and better understand the principles of protein–ligand interactions applicable to rational drug design, we undertook a structural and thermodynamic comparison of biotin and an azobenzene dye bound to streptavidin.

Streptavidin is a tetrameric protein of  $M_r$  64 000 that binds biotin with exceptionally high affinity ( $K_a \approx 10^{13}$  M<sup>-1</sup>).<sup>1</sup> X-ray crystallographic studies of a streptavidin–biotin complex reveal a binding site that is complementary to biotin both in terms of specific hydrogen bonds made to biotin polar atoms and overall steric fit.<sup>2</sup> Organic dyes which differ structurally from biotin also bind to streptavidin. One of these, 2-(4'-hydroxyphenylazo)benzoic acid (HABA), has lower affinity than biotin ( $K_a = 10^4$  M<sup>-1</sup> (Table I)) but is quantitatively displaced when biotin binds, suggesting that both ligands share common binding sites.<sup>1,3</sup> Crystal structures of the streptavidin–biotin and streptavidin–HABA complexes reported here show that the ligands share an important interaction where the biotin ureido and HABA carboxylate oxygens bind in a common oxyanion pocket. Nevertheless, thermodynamic measurements show that the free energy of biotin binding is determined by enthalpy terms, while HABA binding is dominated by entropy.

## Experimental Section

**Crystallographic Studies.** To facilitate structural comparisons between different streptavidin–ligand complexes, X-ray diffraction experiments were carried out with an orthorhombic crystal form,<sup>4</sup> previously used for an independent structure determination of the streptavidin–biotin complex,<sup>5</sup> that allows ligand diffusion into the crystal lattice. Orthorhombic crystals (space group *I*222, dimer per asymmetric unit) of apstreptavidin grown from ammonium sulfate solutions at 30 °C were soaked in saturating concentrations of biotin and HABA to prepare complex crystals.

X-ray data for apstreptavidin, biotin, and HABA complex crystals were collected using a Siemens imaging proportional counter and processed using XENGEN data reduction software.<sup>6</sup> Apstreptavidin unit cell parameters (*a* = 94.2, *b* = 104.0, *c* = 47.7 Å) changed slightly on soaking in ligand solutions (*a* = 95.1, *b* = 105.6, *c* = 47.4 Å, streptavidin–HABA complex; *a* = 95.6 Å, *b* = 105.5 Å, *c* = 47.2 Å, biotin complex). The apstreptavidin  $R_{\text{sym}}$ <sup>7</sup> value for 77 680 observations of 18 543 independent reflections (of 20 189 possible), where the average reflection intensity was greater than the background intensity, was 0.078 to 1.84 Å resolution. The streptavidin–biotin complex  $R_{\text{sym}}$  value for

129 058 observations of 32 621 independent reflections (35 118 possible) was 0.073 to 1.55 Å resolution, where the average intensity of reflections was 2.5 times the background intensity. The streptavidin–HABA complex  $R_{\text{sym}}$  value for 75 101 observations of 18 836 unique reflections was 0.092 to 1.84 Å resolution, where the average intensity of reflections was three times the background intensity.

Structures in the orthorhombic crystal form were determined by molecular replacement, using the biotin complex structure previously determined in space group *I*4<sub>1</sub>22 at 2.6 Å resolution as the probe molecule.<sup>2</sup> Identification of the noncrystallographic symmetry axis relating monomers in the orthorhombic crystal form defined symmetry-constrained rotational searches about the tetramer diad axes, together with translational searches along the unit cell *a* axis.<sup>8</sup> Initial searches in 3 degree and 1 Å increments produced a correlation coefficient of 0.56 using 4–5 Å resolution data, which increased to 0.79 when successively finer increments were searched. Eight cycles of restrained least-squares refinement<sup>9</sup> produced an initial model with a crystallographic *R*-factor<sup>10</sup> of 0.32 for 7036 reflections between 5.0 and 2.5 Å resolution, which was further reduced to *R*-factor = 0.29 using a molecular dynamics refinement protocol.<sup>2</sup>

The high resolution structures of apstreptavidin, and its complexes with biotin and HABA, were refined using restrained least-squares methods,<sup>9</sup> alternating with manual rebuilding cycles into ( $F_o - F_c$ ) $\alpha_{\text{calc}}$  and ( $2F_o - F_c$ ) $\alpha_{\text{calc}}$  electron density maps displayed with the graphics program FRODO.<sup>11</sup> Chemically identical monomers in the crystallographic asymmetric unit were refined independently, starting with ligand-free models. Ligand atoms and solvent molecules were introduced as they emerged as peaks greater than 3 $\sigma$  from the ( $F_o - F_c$ ) $\alpha_{\text{calc}}$  electron density during successive refinement cycles. Refinement parameters for HABA were derived from the crystal structure of 4-(4'-hydroxy-

(1) (a) Chaiet, L.; Wolf, F. J. *Arch. Biochem. Biophys.* **1964**, *106*, 1–5. (b) Green, N. M. *Adv. Protein Chem.* **1975**, *29*, 85–133. (c) Green, N. M. *Methods Enzymol.* **1990**, *184*, 51–67.

(2) Weber, P. C.; Ohlendorf, D. H.; Wendoloski, J. J.; Salemme, F. R. *Science* **1989**, *243*, 85–88.

(3) Green, N. M. *Biochem. J.* **1965**, *94*, 23c–24c.

(4) Pahler, A.; Hendrickson, W. A.; Kolks, M. A. G.; Argarana, C. E.; Cantor, C. R. *J. Biol. Chem.* **1987**, *262*, 13933–13937.

(5) Hendrickson, W. A.; Pahler, A.; Smith, J. L.; Satow, Y.; Merritt, E. A.; Phizackerley, R. P. *Proc. Natl. Acad. Sci. U.S.A.* **1989**, *86*, 2190–2194.

(6) Howard, A. J.; Gilliland, G. L.; Finzel, B. C.; Poulos, T. L.; Ohlendorf, D. H.; Salemme, F. R. *J. Appl. Crystallogr.* **1987**, *20*, 383–387.

(7)

$$R_{\text{sym}} = \frac{\sum_{hkl} \sum_{i=1}^N | \langle I^{hkl} \rangle - \langle I_i^{hkl} \rangle |}{\sum_{hkl} \sum_{i=1}^N I_i^{hkl}}$$

(8) Fujinaga, M.; Read, R. *J. Appl. Crystallogr.* **1987**, *20*, 517–521.

(9) Hendrickson, W. A.; Konnert, J. H. *Biomolecular Structure, Function, Conformation and Evolution*; R. Srinivasan: Oxford, 1980; pp 43–57.

(10) Crystallographic *R*-factor =  $\sum |F_o - F_c| / \sum F_o$ .

(11) Jones, T. A. *J. Appl. Crystallogr.* **1978**, *11*, 268–272.

\* Author to whom correspondence should be addressed.

<sup>†</sup> Current address: Sterling Winthrop Research Division, 9 Great Valley Parkway, Malvern PA 19355.

**Table I.** Thermodynamic Parameters for Streptavidin-Ligand Interactions

ligand	$K_a^a$ (M <sup>-1</sup> )	$n$	$\Delta G^\circ$ (kcal/mol)	$\Delta H^\circ$ (kcal/mol)	$T\Delta S^\circ$ (kcal/mol)	$\chi^2$
HABA	7295 ( $\pm 554$ )	1.12 ( $\pm 0.07$ )	-5.27 ( $\pm 0.05$ )	1.70 ( $\pm 0.01$ )	6.97 ( $\pm 0.04$ )	0.080
HABA <sup>b</sup>	10000		-5.46			
d-biotin <sup>c</sup>	$2.5 \times 10^{13}$	0.86	-18.3	-32.0	-13.7	

<sup>a</sup>Data for average of three experiments (error parameters of  $\pm 1$  standard deviation are in parentheses).  $\chi^2$  gives the average deviation of data points for computed best fit for 18 injection aliquots in each experiment, assuming independent binding sites on the streptavidin tetramer. <sup>b</sup>Literature values for HABA.<sup>1c</sup> <sup>c</sup>Only  $\Delta H^\circ$  and  $n$  were fitting parameters for the observed reaction heat for d-biotin with  $K_a$  fixed at the literature value of  $2.5 \times 10^{13}$  (from ref 1c).

phenylazo)benzoic acid.<sup>12</sup> Aromatic ring geometry was constrained during the protein complex refinement. Planarity constraints were omitted from the azo group linking the HABA aromatic rings.

The apostreptavidin structure (crystallographic  $R$ -factor = 0.209 at 1.84 Å resolution) incorporates 256 water molecules, residues 13–65, 68–133 in molecule 1 and residues 13–46, 52–65, 69–133 in molecule 2 in the crystallographic asymmetric unit (residues 13–138 constitute "core" streptavidin found in commercial preparations<sup>4</sup>). The streptavidin-biotin complex structure ( $R$ -factor = 0.171 at 1.55 Å resolution) incorporates all protein atoms corresponding to residues 13–133 of the mature streptavidin sequence and 209 water molecules. The streptavidin-HABA complex structure was refined to a final crystallographic  $R$ -factor of 0.185 at 1.78 Å resolution. Several residues located at the amino termini or in surface loops (residues 13, 14, 49, 66, 67 in molecule 1 and residues 13, 14, 66–68 in molecule 2 of the asymmetric unit) are poorly defined in the streptavidin-HABA complex and are not included in the model. This model also includes 209 water molecules. Coordinates have been deposited in the Brookhaven Protein Data Bank.<sup>13</sup>

**Calorimetric Studies.** Streptavidin from *Streptomyces avidinii* was purchased from Calbiochem (La Jolla, CA) and used without further purification. HABA and d-biotin were purchased from Fluka (Ronkonkoma, NY) and Sigma (St. Louis, MO), respectively, and used without further purification.

Streptavidin solutions were titrated by addition of  $18 \times 15 \mu\text{L}$  aliquots of ligand solution at 5-min intervals at 25 °C in a MicroCal (Northampton, MA) Omega titration calorimeter.  $K_a$ ,  $\Delta H^\circ$ , and  $n$  (stoichiometry per subunit) were obtained through nonlinear least-squares fit of the observed reaction heat for each titration step.<sup>14</sup> Lyophilized streptavidin was dissolved in unbuffered 100 mM KCl at a concentration of between 4 and 188 mM (Given four biotin binding sites in the streptavidin tetramer, the concentration of ligand binding sites ranged from 15 to 750 mM.) and dialyzed overnight against this same solution. All calorimetry experiments were conducted in 100 mM KCl in the absence of buffer to avoid heat effects due to ionization of buffer components. The pH was adjusted using small amounts of 1 M NaOH and 1 M HCl, and the protein was equilibrated with this solution by dialysis. The pH 6.9 was chosen to insure the full protonation of the phenolic hydroxyl of HABA, as expected from the reported  $pK_a$  of 8.2<sup>15</sup> to 8.5,<sup>16</sup> so that heat effects due to ionization of the ligand are negligible. Furthermore, control experiments where HABA was diluted into 0.1 M KCl and 0.1 M KCl into protein were performed to correct for the small contributions of heat of dilution. Protein concentrations were determined by amino acid analysis, while ligand concentrations were gravimetrically measured. The solid ligands were dissolved in the dialyzate that resulted from the streptavidin dialysis to insure composition identity with respect to all solution components other than the reactants.

For the experiments with HABA it was necessary to use relatively high concentrations of streptavidin (150–188 mM) because of the weak binding and small experimental signal (heat of reaction). The HABA concentration was 10 times that of streptavidin to insure that the observed heats of reaction would be 120–150  $\mu\text{cal}$ /injection at the beginning of the titration and that about 80% of the ligand added per injection was bound by the protein for the first few injections. Moreover, these conditions also insured that about 80% of the binding sites would be satu-

rated after the last injection. The control titration of HABA into 100 mM KCl yielded only  $\sim 3 \mu\text{cal}$ /injection for all 18 injections and indicate that the observed heats of reaction for HABA binding to streptavidin are well above the background signal.

## Results and Discussion

Ligand binding affinity represents the difference in free energy between the protein plus unbound ligand in solution and their complex. As inferred from previous studies at 2.6 Å resolution<sup>2</sup> and verified at high resolution (Figure 1a), streptavidin provides a binding site for biotin whose interactions stabilize a resonance form of biotin which makes better hydrogen bonds with the protein than are possible with biotin in water. This is achieved through polarization of the biotin ureido group so that negative charge is localized on the ureido oxygen (Figure 2). The polarizability of ureas is known from small molecule X-ray studies showing that bond lengths and corresponding atomic charge densities vary in response to the strength of the hydrogen bonding partners.<sup>17</sup> Although expected changes in bond lengths are too small to be reliably determined from the streptavidin-biotin crystal structure, localization of negative charge on the biotin ureido oxygen is reflected by its tetrahedral ( $sp^3$ ) coordination to three protein side chains that donate hydrogen bonds and form an oxyanion pocket for the ureido oxygen (Figure 3). As reported earlier, all of the groups that hydrogen bond to biotin are additionally hydrogen-bonded to other protein groups, forming a rigid lattice that is also present in apostreptavidin.<sup>18</sup>

Additional factors contributing to energetics of ligand binding include favorable entropy effects arising from release of five water molecules ordered in the biotin site of apostreptavidin (including one water with unit occupancy and low  $B$ -value located in the oxyanion pocket) and burying hydrophobic surface area of biotin that was accessible in solution. Opposing entropy effects could arise from biotin immobilization and ordering of loop residues 46–50 on biotin binding.<sup>2</sup> However, the measured free energy of biotin binding to streptavidin ( $\Delta G^\circ = -18.3 \text{ kcal/mol}$ ) is almost wholly enthalpic,  $\Delta H^\circ = -32.0 \text{ kcal/mol}$  (Table I), indicating that net entropy contributions to biotin binding are unfavorable. Taken together, these results suggest that the dominant effect contributing to biotin binding is enhanced hydrogen bonding made between the ligand and protein, due particularly to stabilization of a biotin resonance form whose tetrahedrally coordinated,  $sp^3$  ureido oxygen makes more and stronger hydrogen bonds than an  $sp^2$  oxygen forms with water in solution.

HABA binds streptavidin with minimal alteration of the binding site geometry (Figure 3). This is probably to be expected, given the extensive pattern of binding site interactions outlined previously.<sup>2</sup> HABA is oriented in the binding site so that the position of one of its benzoate oxygen atoms coincides with that of the biotin ureido oxygen, while the remainder of the linked ring system roughly approximates the orientation of the fused biotin rings and aliphatic valeryl side chain (Figures 1 and 3). HABA binding does not completely immobilize the loop comprising residues 46–50 which is disordered in apostreptavidin but becomes immobilized on binding biotin.<sup>2</sup> This loop remains partially disordered in the HABA-streptavidin complex and allows some solvent

(12) Harlow, R. L.; Simons, D. M.; Weber, P. C. *Acta Crystallogr.* **1992**, *C48*, 48–50.

(13) Bernstein, F. C.; Koetzle, T. F.; Williams, G. J. B.; Meyer, E. F., Jr.; Brice, M. D.; Rogers, J. R.; Kennard, O.; Shimanouchi, T.; Tasumi, M. *J. Mol. Biol.* **1977**, *112*, 535–542.

(14) (a) Wiseman, T.; Williston, S.; Brandts, J. F.; Lin, L. *Anal. Biochem.* **1989**, *179*, 131–137. (b) Brandts, J. F.; Lin, L.-N.; Wiseman, T.; Williston, S.; Yang, C. P. *Am. Laboratory* **1990**, *22*, 30–41. (c) Connelly, P. R.; Varadarajan, R.; Sturtevant, J. M.; Richards, F. M. *Biochemistry* **1990**, *29*, 6108–6114.

(15) (a) Baxter, J. H. *Arch. Biochim. Biophys.* **1964**, *108*, 375–383. (b) Thomas, E. W.; Merlin, J. C. *Spectrochim. Acta* **1979**, *35A*, 1251–1255. (c) Ni, F.; Cotton, T. M. *J. Raman Spectrosc.* **1988**, *19*, 429–438.

(16) Green, N. M. *Methods Enzymol.* **1970**, *18A*, 418–424.

(17) Blessing, R. H. *J. Am. Chem. Soc.* **1983**, *105*, 2776–2783.

(18) The oxyanion pocket is analogous to the oxyanion hole in serine proteases (Kraut, J. *Annu. Rev. Biochem.* **1977**, *46*, 331–358) that stabilizes the tetrahedral acyl enzyme intermediate. Both sites incorporate backbone NH groups to indirectly or directly orient hydrogen bond donors toward the oxyanion.

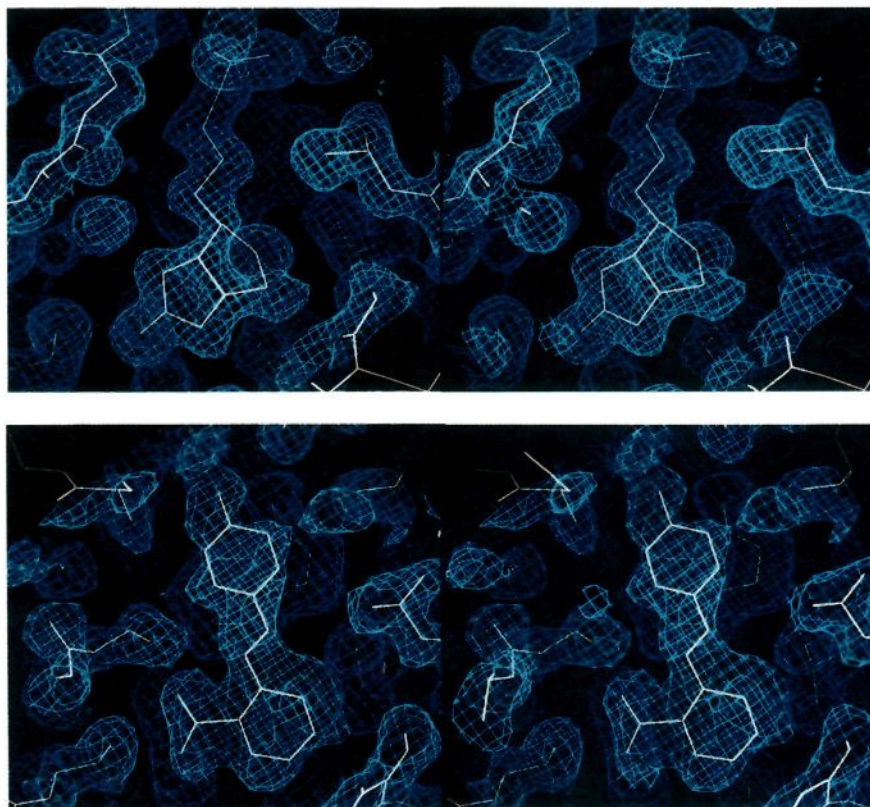


**Figure 1.** Stereoscopic views of  $(2F_o - F_c)\alpha_{\text{calc}}$  electron density for ligands binding to streptavidin: (a, top) biotin at 1.55 Å resolution and (b, bottom) the dye 2-(4'-hydroxyphenylazo)benzoic acid (HABA) at 1.78 Å resolution. Spectroscopic studies indicate that the dye binds as the hydrazone, as also suggested by the tetrahedral character of the azo nitrogen nearest the benzoic acid ring. Less defined electron density for the hydroxyphenyl ring of the dye suggests that it is less constrained than the benzoic acid ring when bound to the protein.

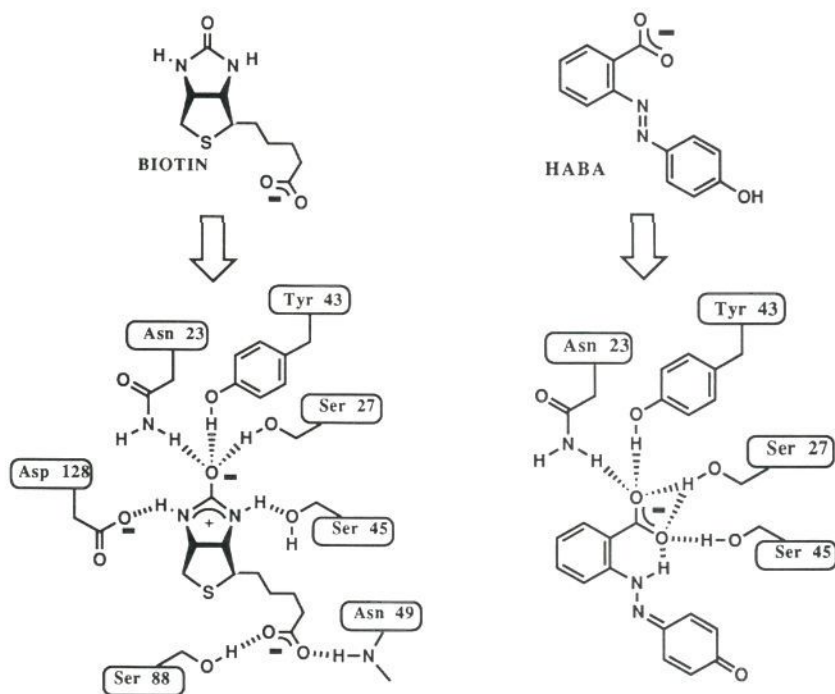


**Figure 2.** Schematic illustrations of biotin (left) and HABA (right) binding to streptavidin. Biotin is bound as a minor resonance form owing to specific protein interactions that polarize the ureido group and allow strong hydrogen bond formation with residues (Asn23, Ser27, Tyr43) in the oxyanion pocket. HABA binds as a hydrazone tautomer, in part because the hydrazone NH proton can stabilize the charge or orientation of the carboxyl group in the hydrophobic environment of the binding site.

exposure of the HABA hydroxyphenyl group, although the same five water molecules that are displaced by biotin are also displaced on HABA binding.

Spectroscopic studies indicate that HABA binds as the hydrazone tautomer, which is favored in low dielectric environments because the hydrazone NH can form an internal hydrogen bond

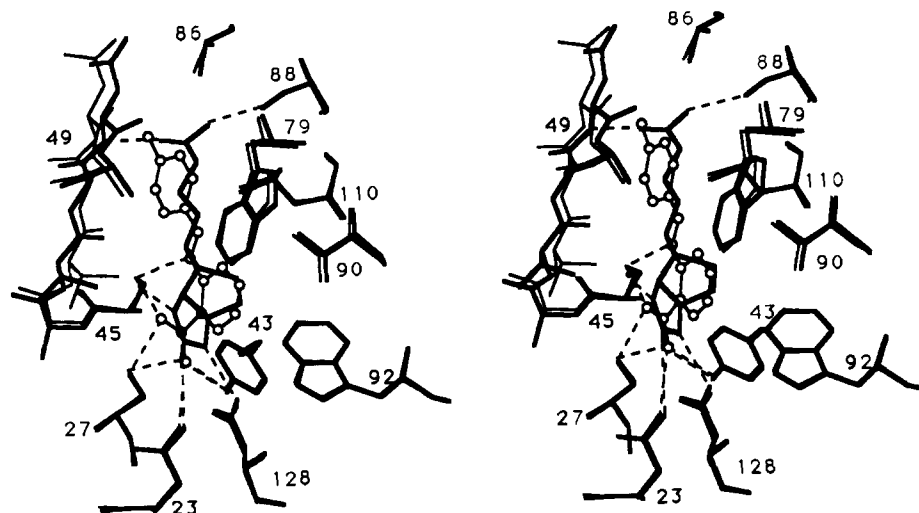


**Figure 3.** Stereoscopic view showing a superposition of the streptavidin-biotin (wider lines) and streptavidin-HABA (thinner lines) complexes. Open circles indicate positions of HABA atoms. Most features of the binding site are conserved despite differences in ligand structure. Minor differences include a small displacement of residues 47–51 in the streptavidin-HABA complex to accommodate the hydroxyphenyl ring of HABA. Thin dashed lines show hydrogen bonds between ligand and protein.

that helps stabilize the benzoate negative charge (Figure 2).<sup>15</sup> Hydrazone binding is consistent with the refined electron density for the ligand (Figure 1b), which shows tetrahedral character at the nitrogen nearest the benzoic acid ring. One benzoate oxygen accepts hydrogen bonds from Asn23, Tyr43, and Ser27 in the oxyanion pocket, while the other shares a hydrogen bond from Ser27 and accepts a hydrogen bond from the hydroxyl of Ser45, together with the internal hydrogen bond from the hydrazone NH (Figure 2). There is no analogue of the biotin-Asp128 interaction in HABA binding, and it is notable that Ser45 reorients so that it donates, rather than accepts, a hydrogen bond to the ligand (Figures 2 and 3). Despite these differences, it is somewhat surprising that HABA binding to streptavidin ( $\Delta G^\circ = -5.27$  kcal/mol (Table I)) is dominated by the entropy terms ( $T\Delta S^\circ = 6.97$  at 25 °C (Table I)). This suggests that despite the preservation of key hydrogen-bond interactions with residues in the oxyanion pocket, hydrophobic interactions predominate in the energetics of HABA binding.

One source of the difference in binding energetics is the extent of ligand polarization possible in biotin versus HABA. Computational estimates of binding energy show substantial increases for biotin resonance forms that localize negative charge on the ureido oxygen and positive charge on the ureido nitrogen atoms,<sup>19</sup>

(19) Point charge distributions for biotin, HABA and HABA hydrazone were computed using a 4-31 basis set and the program GAMESS (Dupius, M.; Spangler, D.; Wendoloski, J. J. NRCC Program QC01). Estimates of ligand-protein interaction energies were made from complex crystal coordinates using the AMBER potential [Weiner, P.; Kollman, P. A. *J. Comput. Chem.* **1981**, *2*, 287–303. Weiner, S. J.; Kollman, P. A.; Case, D. A.; Singh, U. C.; Ghio, C.; Alagona, G.; Weiner, P. *J. Am. Chem. Soc.* **1984**, *106*, 765–784.] for the protein and computed parameters for the ligands. Effects of ligand charge redistribution were estimated by scaling charges on the biotin ureido oxygen-carbon and nitrogen-hydrogen atom pairs to retain local and overall ureido group neutrality. Discounting charge reorganization in the protein, which could be significant, the biotin-streptavidin electrostatic interaction increased 24 kcal/mol per unit excess negative charge localized on the ureido oxygen.

an anticipated result since all of these atoms interact with complementary hydrogen-bond donors or acceptors in the binding site (Figure 2). These interactions underlie streptavidin's ability to stabilize a biotin resonance form that makes more and stronger hydrogen bonds with the protein than the ligand makes with solvent. Although HABA makes geometrically similar interactions with streptavidin, in contrast to biotin there are no resonant charge distributions for the tautomer that produce comparable enhancements in the number or strength of hydrogen bonds that HABA makes to the protein versus solvent. Redistributions of charge in the benzoate carboxyl group that potentially enhance interactions with residues in the oxyanion pocket, for example, attenuate interactions with Ser45, and vice versa. Consequently, while the geometry of the oxyanion binding interactions looks similar for biotin and HABA, their energetics are quite different. Both HABA hydrazone formation and oxyanion pocket interactions reflect a compromise between solution and bound conformations that have little net stabilizing effect on complex formation,<sup>20</sup> while binding is determined by water displacement, hydrophobic forces, and interactions like stacking of the HABA hydroxyphenyl ring with the indole ring of Trp79 (Figures 1b and 3). Most interesting from the drug design standpoint are the fundamental differences in energetics and driving forces for the natural and "screened" ligand. Although this is an implicit assumption of many mechanism-based or structural approaches to ligand design, it seems clear that very different energetics frequently accompany structurally similar protein-ligand interactions.<sup>20</sup> At the same time, plausible strategies for increasing affinity of the HABA "lead compound" may be successful, although they exploit the unique properties of the streptavidin binding site in ways that are different, if not as ultimately effective as the natural ligand.

(20) Morgan, B. P.; Scholtz, J. M.; Ballinger, M. D.; Zipkin, I. D.; Bartlett, P. A. *J. Am. Chem. Soc.* **1991**, *113*, 297–306.